

## Identification of a Tumor-Suppressive Human-Specific MicroRNA within the *FHIT* Tumor-Suppressor Gene

Baocheng Hu<sup>1,5</sup>, Xiaomin Ying<sup>2</sup>, Jian Wang<sup>5</sup>, Jittima Piriyaopongsa<sup>8</sup>, I. King Jordan<sup>6</sup>, Jipo Sheng<sup>1</sup>, Fang Yu<sup>1</sup>, Po Zhao<sup>3</sup>, Yazhuo Li<sup>3</sup>, Hongyan Wang<sup>5</sup>, Wooi Loon Ng<sup>5</sup>, Shuofeng Hu<sup>2</sup>, Xiang Wang<sup>5</sup>, Chenguang Wang<sup>7</sup>, Xiaofei Zheng<sup>4</sup>, Wujun Li<sup>2</sup>, Walter J. Curran<sup>5</sup>, and Ya Wang<sup>5</sup>

### Abstract

Loss or attenuated expression of the tumor-suppressor gene *FHIT* is associated paradoxically with poor progression of human tumors. *Fhit* promotes apoptosis and regulates reactive oxygen species; however, the mechanism by which *Fhit* inhibits tumor growth in animals remains unclear. In this study, we used a multidisciplinary approach based on bioinformatics, small RNA library screening, human tissue analysis, and a xenograft mouse model to identify a novel member of the miR-548 family in the fourth intron of the human *FHIT* gene. Characterization of this human-specific microRNA illustrates the importance of this class of microRNAs in tumor suppression and may influence interpretation of *Fhit* action in human cancer. *Cancer Res*; 74(8); 2283–94. ©2014 AACR.

### Introduction

The *FHIT* (fragile histidine triad) gene was identified in 1996 at *FRA3B* (1) that is well known as the most activated common fragile region. Common fragile sites in the chromosome regions are more susceptible to breakage, rearrangements, and deletions than other sites in the genome. *FHIT* is frequently lost in different types of human tumors due to the alteration of *FRA3B*. Since *FHIT* was identified, several hundred scientific articles have been published to report *FHIT* deletion, low expression, or promoter methylation in the majority of human cancers (2–7). It was also reported that *Fhit*-deficient mice developed more tumors (8). The association of *Fhit* to cancer was related to *Fhit* in promoting apoptosis and regulating the production of the reactive oxygen species (9–12). These discoveries demonstrate that *FHIT* is a tumor suppressor. How-

ever, the results pertaining to the inhibitory effects of up-regulated *Fhit* on tumor growth are controversial (13–16), suggesting that additional mechanisms need to be elucidated. The *FHIT* coding region distributing over 10 exons (~1,100 base pairs, bp) encodes an approximately 17-kD protein but the entire gene including noncoding portion with 9 introns is around 1.5 Mb. Because misregulated microRNAs (miRNA) involved in cancer are frequently located at fragile sites (17), we were interested in exploring whether the *FHIT* gene encoded any miRNA with an effect on inhibiting tumor growth. As a result, we identified a novel miRNA in *FHIT* intron 4, and found that this miRNA is a new member of the miR-548 family.

The miR-548 family is primate/human-specific (18) and derived from repetitive elements in the genome (19). Until now, 68 members of the hsa-miR-548 family have been documented in the miRBase database of miRNA sequences (<http://www.mirbase.org/>; not including the one described in this study; Supplementary Table S1). The hsa-miR-548 is derived from *Made1* transposable elements that are short miniature inverted-repeat transposable elements (MITE) and consist of two 37-bp terminal inverted repeats that flank 6 bp of the internal sequence. Thus, *Made1* elements are nearly perfect palindromes, and when expressed as RNA they form highly stable hairpin loops. Apparently, these *Made1*-related structures are recognized by the RNA interference enzymatic machinery and are processed to form approximately 22-bp mature miRNA sequences. The evolutionary lineage-specific nature of MITEs also provides for a generation of novel regulatory phenotypes related to species diversification. Similar to all other members of the family, the novel member expresses also relatively low when compared with most miRNAs in the human genome; however, the miR-548 family may contain >1,000 members (as predicted and supported by this study). Our data showed that this new member in *FHIT* intron could have an accumulative function with multiple members of the miR-548 family toward inhibiting tumor cell growth.

**Authors' Affiliations:** <sup>1</sup>Department of Medical Molecular Biology, Beijing Institute of Biotechnology; <sup>2</sup>Center of Computational Biology, Beijing Institute of Basic Medical Sciences; <sup>3</sup>Department of Pathology, Chinese PLA General Hospital; <sup>4</sup>Department of Biochemistry and Molecular Biology, Beijing Institute of Radiation Medicine, Beijing, China; <sup>5</sup>Department of Radiation Oncology, Emory University School of Medicine, Winship Cancer Institute of Emory University; <sup>6</sup>School of Biology, Georgia Institute of Technology, Atlanta, Georgia; <sup>7</sup>Department of Cancer Biology, Kimmel Cancer Center, Thomas Jefferson University, Philadelphia, Pennsylvania; and <sup>8</sup>Genome Institute, National Center for Genetic Engineering and Biotechnology, Pathumthani, Thailand

**Note:** Supplementary data for this article are available at Cancer Research Online (<http://cancerres.aacrjournals.org/>).

B. Hu, X. Ying, and J. Wang contributed equally to this article.

**Corresponding Authors:** Ya Wang, Emory University, 1365 Clifton Rd, Suite C5090, Atlanta, GA 30322. Phone: 404-778-1832; Fax: 404-778-1750; E-mail: ywang94@emory.edu; and Baocheng Hu, Department of Medical Molecular Biology, Beijing Institute of Biotechnology, Beijing 100850, China. Phone: 86-10-8817-8372; Fax: 86-10-6824-8045; E-mail: baochenghu@yahoo.com.cn

doi: 10.1158/0008-5472.CAN-13-3279

©2014 American Association for Cancer Research.

These results not only help us understand the function of the *FHIT* gene as a tumor suppressor but also reveal an important role of the unique miR-548 family in inhibiting human cancer development.

## Materials and Methods

### Prediction of the candidate miRNAs in the *FHIT* introns

The nine introns of the *FHIT* gene were extracted from the UCSC genome browser (20). An ensemble classifier termed ABmiPred was constructed (21) using machine learning methods. A total of 300 miRNA precursors (pre-miRNA) were randomly selected from miRBase for positive training samples. A total of 44,500 pseudo pre-miRNAs were randomly selected from 57,994 pseudo pre-miRNAs derived from human 3'UTR (untranslated region) sequences for negative training samples. The secondary structures of the *FHIT* introns were predicted using an RNAfold (22) in windows of 1,000 nucleotides with an overlap of 150 nucleotides. After removing the hairpins with minimum free energy (MFE) greater than  $-15$  kcal/mol, 3,440 hairpins were obtained. Among them, 190 hairpins were predicted as pre-miRNA candidates at a threshold of 0.5 with known miRNAs (miRBase release 13; ref. 23), fRNAdb3 (24), and NONCODE2 (25), which homologous sequences were compared using Basic Local Alignment Search Tool (BLAST). Finally, four predicted pre-miRNA candidates that were homologous to *bona fide* miRNAs and conserved noncoding regions were taken as our miRNA candidates.

### Plasmids construction and packaging

To construct a plasmid expressing the new member of the miR-548 family and other miRNAs, we amplified the pre-miRNA with 100-bp context flanked sequence on each side using the human genomic DNA (Promega) with the different primers (Supplementary Table S4) according to the procedure described previously (26). The amplified fragment was first cloned into a PCR cloning vector and subsequently into pIRES2-EGFP (Clontech) at *Bam*H I and *Sal* I sites and the lentiviral vector pCDH-CMV-MCS-EF1-copGFP (System Biosciences) at the *Eco*R I and *Bam*H I sites. The plasmid packaging was as described previously (26). The luciferase-UTR reporter plasmid that contains the 3'UTR of *CCND1*, *ERBB2*, *DNMT3A*, or *DNMT3B* that carry a putative new miRNA-binding site or a deleted mutant without the new miRNA-binding site was constructed with the complementary oligonucleotides (Supplementary Table S4) and inserted into a modified pGL3-control plasmid firefly luciferase vector (Promega).

### Northern blot

The total RNA was extracted from 293FT or HeLa cells. Twenty microgram of total RNA was separated in 1% of agarose gel (containing 50  $\mu$ g ethidium bromide in 100 mL gel). The RNA marker was purchased from Sigma-Aldrich Inc. After transferring to a nylon membrane (GE Healthcare), the membrane was hybridized with a special probe, 5'-GTTGCCATTA CTTTCAAGGGCAAAAACCATAGTTACTTTTGTACCAATCT-GATATTTTTCTTCCAA-3'-Dig (for detecting the pri-miRNA at chromosome 1, chr1), or 5'-TTAGCTTGGTGCAAAAGTAAC

TATGGTTTTTGGGCAAAAACCATAGTTACTTTTGCACCAATCTAA-3'-Dig (for detecting the pri-miRNA at chromosome 3, chr3). The membrane was soaked in a solution containing the DIG antibody and followed a procedure according to the manufacturer's instructions (DIG Wash and Block Buffer Set; Roche). The signals were obtained by exposing the membrane to X-ray films at room temperature.

### Human cell lines and tissue samples

Human cell lines: 293FT (transformed embryo kidney cells), MRC-5 (fetal lung fibroblast cells), BJ cell (immortalized fibroblast cells), HeLa (cervical cancer cells), U87MG (brain tumor cells), HT29 (colon cancer cells), H144 (melanoma cells), A549 (lung cancer cells), H1299 (lung cancer cells), and H1975 (lung cancer cells) were purchased from American Type Culture Collection 10 years ago. A2780 (ovarian cancer cells) were obtained from the European Collection of Cell Cultures 6 years ago. L02 (liver cells) were obtained as described previously (27). 3KT (hTERT-immortalized cells) were obtained from Dr. Jerry Shay's laboratory (University of Texas Southwestern Medical Center, Dallas, TX; ref. 28). M059J and M059K (brain tumor cells) were obtained from Dr. Allalunis-Turner's laboratory (University of Alberta, Alberta, Canada; ref. 29). The lung cancer cell lines, 95C and 95D, were obtained from Dr. Yinglin Lu's laboratory (Chinese PLA General Hospital, Beijing, China) as described previously (26). The other human lung cancer cell lines (H460, H358, H157, H1792, Calu1, H266B, and SK-MES-1) were obtained from Dr. Shi-Yong Sun's laboratory (Emory University School of Medicine, Atlanta, GA; ref. 30). All the human cell lines were tested within 6 months before starting this project by subcutaneously injecting individual one into nude mice (three injections for one cell line) to confirm whether they were tumorigenic at 30 days after injection. Human lung tissues were obtained from the pathology facility at Emory (30 pairs) and from the Department of Pathology, at the PLA General Hospital, Beijing, China (15 pairs).

### Xenograft mouse model

The animal protocol was approved by the Emory University Institutional Animal Care and Use Committee (IACUC). The experiment was carefully performed following Emory University IACUC guidelines for animal care. Similar to our previous report (26), both hind legs of each nu/nu mouse (male, 2-month-old, bodyweight  $\sim 22$  g, purchased from The Jackson Laboratory) were subcutaneously injected with  $3 \times 10^6$  human tumor cells transfected with vector alone or with the vector encoding the purposed miRNA or genes as described above, or transfected with vector alone or the vector encoding *FHIT* as previously described (31), 5 mice for each group. The mice were sacrificed at 30 days after the tumor cell inoculation and the tumors were removed and weighed.

### Statistical analysis

Statistical analysis of data between two groups was done using the Student *t* test or the Mann-Whitney *U* test when a normal distribution could not be assumed. One-way ANOVA was used for multiple group comparisons. The correlation coefficients were analyzed by Spearman's  $\rho$ . Statistical



subcloned the PCR product of C2-miRNA into pMD18-T, sequenced, and analyzed it. These results verified that C2-miRNA (with 22 nucleotides, nt) is a novel miRNA and belongs to the miR-548 family as it is similar to 2 members of the miR-548 family, miR-548d-5p and miR-548d-3p (Fig. 1D and Supplementary Table S1).

When performing a complete human genomic sequence search, we found that there was another identical 22 nt sequence (C2-miRNA\*) on Chr1 in addition to Chr3 (*FHIT* gene located; Supplementary Fig. S1D). Although the extended sequence on chr1 could not form a pre-miRNA (stem loop) structure, to exclude any possibilities that make the sequence expression, we compared the stably expressing levels of the two constructs (containing the 22 nt on Chr1 or Chr3 with ~100-bp context flanked sequence on each side) in 293FT, A549, H1299, and HeLa cells (Supplementary Figs. S1D and S1E). The results showed that the Chr3 construct highly expressed but the Chr1 construct did not express in these cell lines (Fig. 1E), supporting that chr3 (the *FHIT* intron) is the function location of the new miRNA. The Northern blot data provide additional evidence to support the conclusion (Fig. 1F). Also, both strands of C2-miRNA expressed similarly (Supplementary Fig. S1F), suggesting that both C2-miRNA (5p) and C2-miRNA\* (3p) functionally work on their targets. Furthermore, we generated a small RNA library from 293FT (Fhit-positive) and HeLa (Fhit-negative) cells, and did a deep-sequence comparison between the detected small RNAs from the two cell lines (LC Sciences Inc., see the Supplementary Methods). The results showed that both the cDNA sequences of mature C2-miRNA and C2-miRNA\* on the chr3 region were detected in 293FT cells but not in HeLa cells; and the sequences on the chr1 region were not detected in either 293FT cells or HeLa cells. These data confirm that C2-miRNA in the *FHIT* intron is a real miRNA.

#### C2-miRNA and Fhit are under the same transcriptional control

We compared the expression levels of the C2-miRNA and *FHIT*/Fhit in 45 pairs of human lung tumors and their adjacent nontumor tissues (30 pairs of samples from the Emory pathology facility and 15 pairs of samples from the PLA General Hospital pathology facility in China), as well as 24 human cell lines, including 5 from normal and 19 from tumors using quantitative RT-PCR (qRT-PCR) and a Western blot assay. The results showed that similar to the expression trend of the *FHIT* mRNA, the relative level of C2-miRNA was lower in 32 tumor samples than in their nontumor counterparts (Fig. 2A). The correlation of the *FHIT* mRNA expression and the C2-miRNA expression is significant ( $P = 0.006$ ). In addition, both C2-miRNA and Fhit expressed relatively low in most human tumor cell lines when compared with in normal cell lines (Fig. 2B and C), suggesting that C2-miRNA, located in the intron of *FHIT*, was controlled by the same promoter of *FHIT*.

To verify that C2-miRNA and the *FHIT* mRNA were controlled by the same promoter, we examined the effects of some promoter modifications on the expression of C2-miRNA and the *FHIT* mRNA. First, we used 5-Aza-2<sup>1</sup>-deoxycytidine

(5-AZA), a DNA methylation inhibitor (33), to treat the lung cancer cell line, H1299, and then measured the levels of the *FHIT* mRNA and C2-miRNA using qRT-PCR because it was reported that the Fhit expression increased in the cell line after 5-AZA treatment (34). The results showed that after the cells were treated with 5-AZA, both the levels of the *FHIT* mRNA and C2-miRNA increased with a similar ratio (Fig. 2D). We then upregulated TNF- $\alpha$ , one of *FHIT* transcription factors, to stimulate *FHIT* expression in 293FT cells and measured the levels of the *FHIT* mRNA and C2-miRNA. SOD2, a known transcriptional target of TNF- $\alpha$ , was used as a positive control. The results showed that TNF- $\alpha$  stimulated the levels of the *FHIT* mRNA and C2-miRNA with a similar ratio (Fig. 2E). These results strongly support that C2-miRNA and *FHIT* are under the same transcriptional control. However, we did find that the levels of mature C2-miRNA were much lower than the levels of the *FHIT* mRNA in the same samples.

To study whether any mutation resulted in the low expression level of C2-miRNA, we performed a detailed search in *FHIT*, including intron 4 (C2-miRNA location), using the University of Santa Cruz (UCSC) Genome Browser (hg19) with the Catalogue of Somatic Mutations in Cancer (COSMIC) database from the Sanger catalogue of somatic mutations in The Cancer Genome Atlas from the National Cancer Institute (35). The results showed that *FHIT* contains 25 somatic substitutions and 9 break points, and intron 4 contains 1 somatic substitution and 3 break points (Supplementary Figs. S2A and S2B). There is a common marked single-nucleotide polymorphism (SNP): "A" or "C" in pre-C2-miRNA but no mutation is found around the C2-miRNA region (Supplementary Fig. S2C). After sequencing the pre-C2-miRNA region in four cell lines (293FT, HT-144, DU145, and H157), we found two of them (293FT and H157) with "A" and two of them (DU145 and HT-144) with "C" (Supplementary Fig. S2D), confirming that this SNP is common. We also showed that neither the "A" SNP nor the "C" SNP affects the mature C2-miRNA expression (Supplementary Fig. S2E). These results exclude the possibility that any mutation in pre-C2-miRNA results in the low expression of C2-miRNA.

#### The miR-548 family, including C2-miRNA, showed an inefficient maturation process

Considering the low expression is a common characteristic among all the members of the miR-548 family, we hypothesized that the actually low expression of the miR-548 family, including C2-miRNA, is due to an inefficient maturation process. To test this hypothesis, we first made several standard curves of *FHIT* cDNA, pri-C2-miRNA, mature C2-miRNA, pri-miR-21, and mature miR-21 using different amounts of mimics, plasmid encoding *FHIT* cDNA (31) or pri-miRNAs by qRT-PCR (Supplementary Fig. S3A). On the basis of the standard curves, we compared the endogenous expression levels of C2-miRNA and *FHIT* in 293FT cells and A549 cells. The results showed that the expression percentage of C2-miRNA to *FHIT* cDNA in 293FT cells is 1.6% (Fig. 3A and Supplementary Table S2), confirming that the endogenous mature C2-miRNA level was much lower than Fhit in human cells and suggesting that the low C2-miRNA level might be due to an inefficient maturation

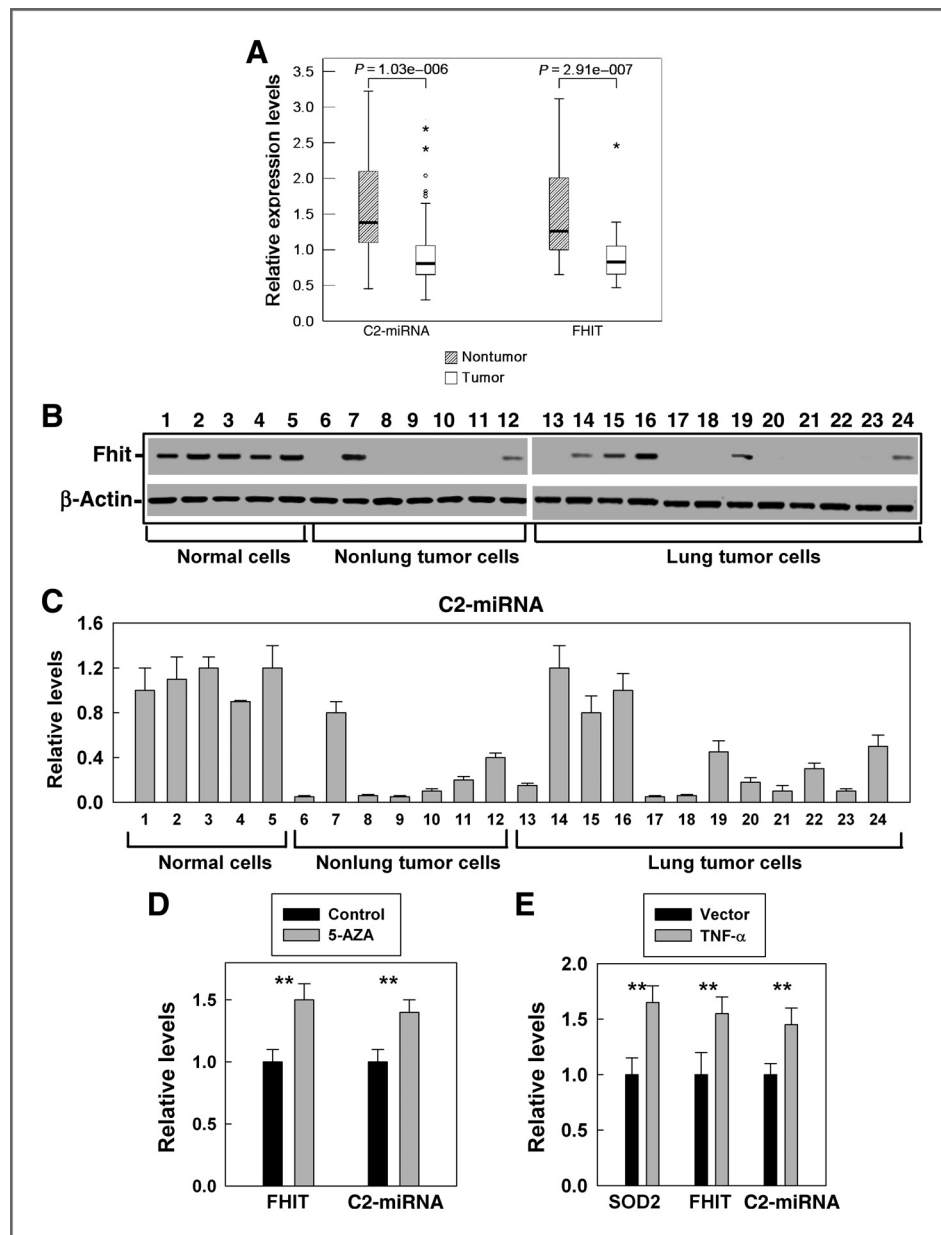


**Figure 2.** The levels of *FHIT*/*Fhit* and C2-miRNA showed a similar expression trend in human tissue and cell lines. **A**, the relative levels of the *FHIT* mRNA or C2-miRNA expression in 45 pairs of human lung tumor tissue and adjacent nontumor tissue samples were measured using a qRT-PCR. Each point of the relative levels of the *FHIT* mRNA or C2-miRNA in lung tumor and adjacent nontumor tissue samples represent the mean of six measurements (two triple sets) from two independent experiments. **B**, the *Fhit* levels were examined in human cell lines, including 5 normal and 19 tumor cell lines, using a Western blot assay. Normal cells: 1, 3KT; 2, BJ; 3, L020; 4, MRC-5; 5, 293FT. Tumor cells: 6, HeLa; 7, H144; 8, M059J; 9, M059K; 10, U87MG; 11, HT29; 12, A2780; 13, H157; 14, H460; 15, A549; 16, H358; 17, 95C; 18, 95D; 19, SK-MES-1; 20, H1792; 21, H1299; 22, Calu-1; 23, H1975; 24, H226B. **C**, relative levels of C2-miRNA were examined in the cell lines as described in **B** using a qRT-PCR assay (*FHIT* data not shown). Each point represents the mean of six measurements (two triple sets) from two independent experiments. **D**, human tumor cells (H1299) were treated with 1  $\mu$ mol/L of 5-AZA (Sigma-Aldrich Inc.) for 48 hours. A qRT-PCR assay was performed with the *FHIT* or C2-miRNA primers (Supplementary Table S4). Data, mean  $\pm$  SD from two independent experiments (two triple sets), \*\*,  $P < 0.01$ . **E**, 293FT cells were transiently transfected with 1  $\mu$ g of vector alone or the vector encoding TNF- $\alpha$ . At 48 hours after transfection, the cells were collected and total RNAs were extracted for a qRT-PCR assay with the SOD2 (a positive control as described in our previous publication; ref. 45). Data, mean  $\pm$  SD from two independent experiments (two triple sets); \*\*,  $P < 0.01$ .

process because we already showed the same transcription regulation of the *FHIT* mRNA and C2-miRNA (Fig. 2D and E).

We then compared the exogenous C2-miRNA and miR-21 in 293FT cells after the cells were transfected with the same

molecular amount of the plasmid encoding an extended pre-miRNA with 100-bp context flanked sequence on each side (Fig. 3B) by using the standard curves (Supplementary Fig. S3A). The results showed that although the exogenous pri-C2-

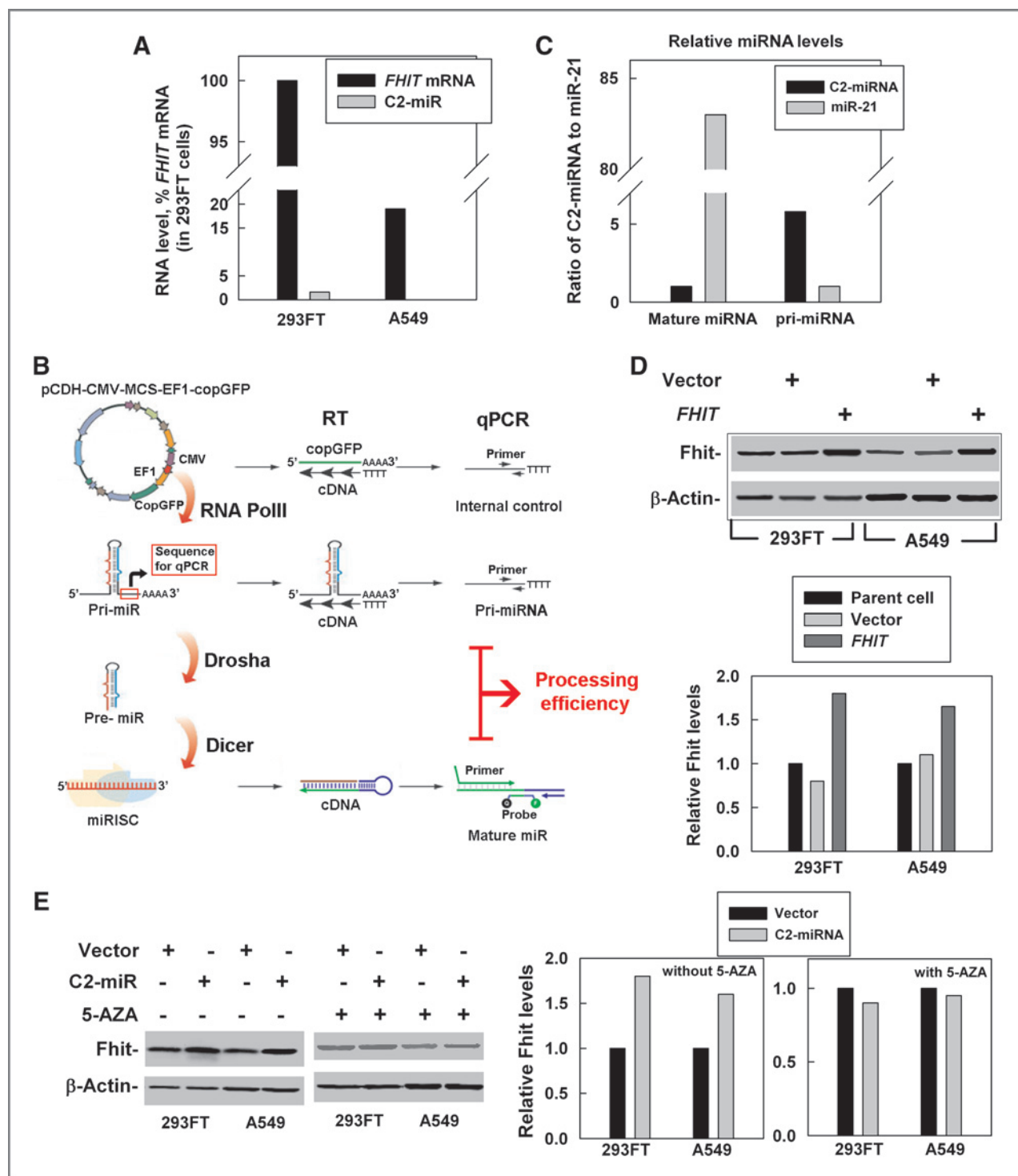


**Figure 3.** C2-miRNA and *FHIT* are under the same transcriptional control. **A**, relative copy numbers of *FHIT* and C2-miRNA in 293FT cells or A549 were calculated based on the curves shown in Supplementary Fig. S3A. **B**, outline of the approach to detect the pri-miRNA or mature miRNA in 293FT cells. The framed part in pri-miRNA indicates the sequences of pri-C2-miRNA or pri-miR-21 that were amplified by qRT-PCR. **C**, the levels of mature miRNAs or pri-miRNAs were measured in 293FT at 24 hours after the cells were transfected with the GFP vector (pCDH-CMV-MCS-EF1-copGFP), encoding pri-C2-miRNA or pri-miR-21 by qRT-PCR. The transfection efficiency was normalized by the GFP signals. The detailed values were shown in Supplementary Table S3. **D**, top, the Fhit protein levels were measured by using a Western blot from 293FT and A549 cells transfected with the vector alone or vector encoding *FHIT*.  $\beta$ -Actin was used as an internal loading control. Bottom, the protein levels (top) were quantified by an application software version 3.0 in Odyssey Infrared Imaging System from LI-COR Biosciences Company. **E**, left, the Fhit protein levels from 293FT and A549 cells transfected with the vector alone or vector encoding C2-miRNA (as shown in Fig. 1E), treated with or without 5-AZA for 48 hours. Right, the protein levels (left) were quantified as described in D.

miRNA levels were higher (~6-fold) than the exogenous pri-miR-21 levels (Supplementary Table S3), the exogenous mature C2-miRNA levels were much lower than the exogenous mature miR-21 (roughly a ~83-fold difference) in 293FT cells (Fig. 3C and Supplementary Table S3). Similar results (highly pri-miRNA levels but lowly miRNA levels) were observed in other 2 members of the miR-548 family: miR-548d and miR-548e (data not shown). These results indicate that the low expression of C2-miRNA is not due to an inefficient transcription but is related to an inefficient mature process for generating mature C2-miRNA, suggesting that the low expression of miR-548 family is through a same mechanism.

We next examined the effects of overexpressing *FHIT* cDNA or C2-miRNA on the levels of C2-miRNA or Fhit/*FHIT*. The results showed that overexpressing the coding region of *FHIT* did not affect the C2-miRNA level (Supplementary Fig. S3B); however, upregulating C2-miRNA clearly increased the Fhit expression level (Fig. 3E). After the cells were treated with 5-AZA, the C2-miRNA-stimulated *FHIT*/Fhit expression disappeared (Fig. 3E and Supplementary Fig. S3C), which indicates that the effects of C2-miRNA on promoting the Fhit expression are involved in demethylation of the *FHIT* promoter, suggesting that C2-miRNA targets some methylation enzymes.

#### C2-miRNA inhibited human tumor cell growth *in vitro* and *in vivo* (xenograft mouse model)

To examine whether C2-miRNA has any function to affect tumor growth, we used three human tumor cell lines: HeLa (without Fhit expression), A549 (with normal Fhit expression), and H1299 (with low Fhit expression) that were overexpressed with pri-C2-miRNA or the control vector (Fig. 1E). The cell transfection efficiency was observed with the GFP signals (Supplementary Fig. S4A), and the C2-miRNA expression levels were as described by qRT-PCR (Fig. 1E, C2-miR-Ch3). We then examined the tumor cell growth. At the same time, we also included the HeLa cells overexpressed with Fhit (31) because it was previously reported that upregulating Fhit expression in HeLa cells did not inhibit HeLa cell growth *in vitro* (tissue culture) and *in vivo* (xenograft mouse model; ref. 15). The results showed that after C2-miRNA was upregulated in these human tumor cell lines (Fig. 1E and Supplementary Fig. S4A), the tumor cell growth was much slower than their vector alone or *FHIT* cDNA-transfected counterparts (Fig. 4A–C). Notably, the effects of C2-miRNA on cell growth inhibition were abolished when the cells were treated with the C2-miRNA inhibitor (22 nt antisense of C2-miRNA) but not affected with a control RNA (22 nt; Fig. 4A–C), supporting the specific inhibition effects of C2-miRNA on tumor cell growth. On the other hand, the apoptosis ratio had no significant difference among these cell lines without any stress stimulation (Fig. 4D), excluding the possibility that C2-miRNA-inhibiting tumor cell growth is through promoting apoptosis. The *FHIT* cDNA overexpression in HeLa cells did not dramatically affect the xenograft size and weight (Fig. 4E), which was similar to that previously reported (15); however, C2-miRNA overexpression significantly suppressed HeLa cell growth *in vitro* and *in vivo* (Fig. 4C and E). The immunohistochemistry data showed that the Ki67 signal (a marker for cell proliferation) but not the caspase-3

signal (a marker for cell apoptosis) was greatly decreased in the xenograft tumor derived from HeLa cells overexpressed with C2-miRNA but not with Fhit (Supplementary Fig. S4B). These results support that C2-miRNA but not Fhit could inhibit tumor cell growth.

#### C2-miRNA inhibited human tumor growth through targeting *CCND1*, *ERBB2*, *DNMT3A*, and *DNMT3B*

To look for the C2-miRNA targets related to the stimulated tumor growth, we focused on cyclin D1 (encoded by the *CCND1* gene), ErbB2 (encoded by the *ERBB2* gene), DNMT3A, and DNMT3B. The reasons for picking up these genes are as follows: (i) We previously found that the expression of Fhit and cyclin D1 (encoded by the *CCND1* gene) was significantly opposite in human cholangiocarcinoma (36); (ii) It was reported that the 3'UTR of *ERBB2* had a binding site for miR-548d-3p (one member of the miR-548 family; ref. 37); (iii) C2-miRNA promoted Fhit expression through demethylating the *FHIT* promoter (Fig. 3 and Supplementary Fig. S3C); (iv) miRNAs targeting *CCND1*, *ERBB2*, or *DNMT3A/DNMT3B* could inhibit tumor growth (38–41); (v) the 3'UTR of *CCND1*, *ERBB2*, *DNMT3A*, or *DNMT3B* has potential binding site of C2-miRNA/C2-miRNA\* (Supplementary Fig. S5A). The luciferase assay verified that these potential sites at 3'UTR of these genes were the real ones for C2-miRNA/C2-miRNA\* binding (Fig. 5A) and the Western blot data further confirmed that *CCND1*, *ERBB2*, *DNMT3A*, and *DNMT3B* are C2-miRNA targets (Fig. 5B, lanes 1 and 2). Also, the relatively high level of cyclin D1 or ErbB2 in the human lung tumor samples with a low expression of C2-miRNA (Supplementary Fig. S5B), and the effects of the C2-miRNA inhibitor on the expression levels of these targeted genes provide additional evidence for C2-miRNA targeting these genes (Fig. 5B, lanes 3 and 4).

To examine whether the inhibitory effects of C2-miRNA on tumor growth were related to targeting *CCND1*, *ERBB2*, *DNMT3A*, or *DNMT3B*, we overexpressed the *CCND1*, *ERBB2*, *DNMT3A*, or *DNMT3B* without 3'UTR in the tumor cells that already overexpressed with C2-miRNA and observed the sizes of the xenograft derived from these cells. The results showed that transfecting *CCND1*, *ERBB2*, *DNMT3A*, or *DNMT3B* without 3'UTR into the tumor cells that already overexpressed with C2-miRNA could successfully upregulate the levels of cyclin D1, ErbB2, DNMT3A, or DNMT3B (Fig. 5B, lanes 5 and 6; Supplementary Fig. S5C) and partially reversed the inhibitory effects of C2-miRNA on the tumor cell growth *in vitro* (Supplementary Fig. S5D) and *in vivo* (Fig. 5C). These results strongly support that the role of C2-miRNA in inhibiting tumor cell growth is associated with targeting *CCND1*, *ERBB2*, or *DNMT3A/DNMT3B*.

#### The accumulative effects of the miR-548 family, including C2-miRNA, on targeting oncogenes and inhibiting tumor development

The endogenous level of C2-miRNA, similar to the other members of the miR-548 family, is relatively low in human cells; however, the members of the family share very conservative sequence at the targeting gene region (19) and it is known that multiple miRNA could target one mRNA in clusters or different

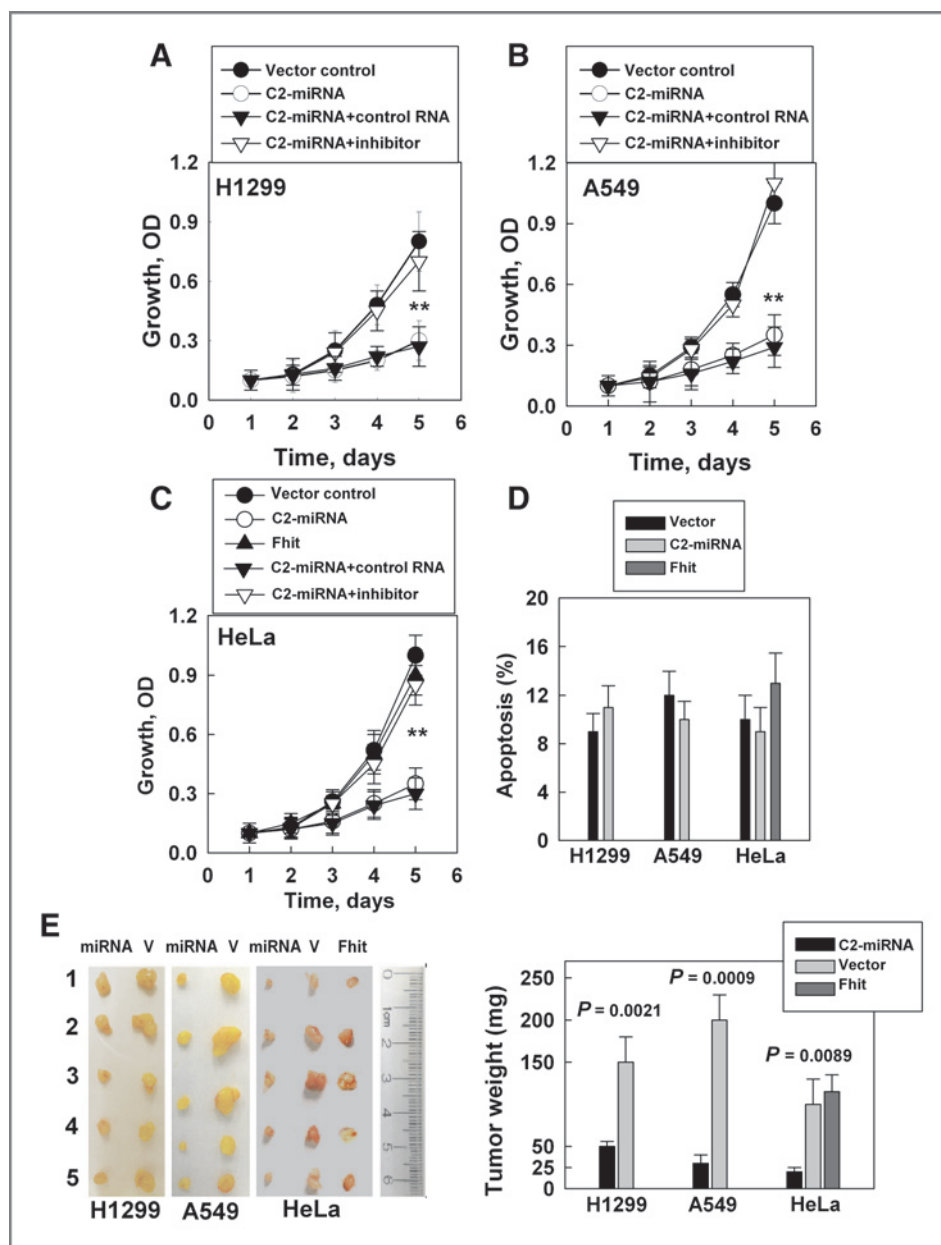


**Figure 4.** C2-miRNA inhibits human tumor cell growth. H1299 (A), A549 (B), HeLa (C) cells stably expressed with either vector alone or the vector encoding pre-C2-miRNA as described in Fig. 1E were plated in 96-well plates for a cell viability assay. At 24 hours later, the cells were treated with 30 nmol/L of control RNA (22 nt) or the C2-miRNA inhibitor (22 nt antisense of C2-miRNA) for an additional 24 hours. The MTT assay was performed. Data, mean  $\pm$  SD from two independent experiments with triple samples for each experiment, \*\*,  $P < 0.01$ . D, apoptosis was measured using flow cytometry with an Annexin V-PE Apoptosis Analysis Kit. Data, mean  $\pm$  SD from three independent experiments. E, left, xenografts were derived from A549 or H1299 transfected with control RNA or C2-miRNA, or from HeLa cell lines transfected with vector alone, overexpressed with C2-miRNA or *FHIT*. Right, analyzed the tumor weight. The tumors were weighed and the data represent mean  $\pm$  SD from 5 tumors for each cell line.

locations (42), we were interested in study whether the members of the miR-548 family could cooperate together to inhibit human tumor growth. To test the hypothesis, we first requested NanoString Inc. with the available color probes to measure the levels of 19 members of the miR-548 family that covered 29 mature members in the family (Supplementary Table S5) and miR-21 (as a control) in 30 pairs of human lung tissues and 24 human cell lines using their sensitive technology (Supplementary Fig. S6A; ref. 43). Because each individual member of the miR-548 family expressed relative low, we accumulated the total expression levels from all the miR-548 family members as one count from each sample and compared the ratio of the miR-548 family levels in tumor tissue/cells and in their nontumor counterparts. The results showed that the

relative levels of the miR-548 family were lower in most tumor tissue or tumor cells than in their nontumor counterparts (Fig. 6A and B), which is similar to that of C2-miRNA in these samples (Fig. 2), suggesting that the members of the miR-548 family, including C2-miRNA, may work together to play an accumulative role in inhibiting human tumor development. Our qRT-PCR data verified the accuracy of NanoString's measurement (Fig. 6C and Supplementary Fig. S6A). These results confirm the expression levels of the miR-548 family that we measured in human tumor tissue and cells.

To explore the importance of the miR-548 family, we predicted the total numbers of the miR-548 family in the human genome. Considering both sequence and structural requirements for miRNA, 1,182 putative sequences were found with

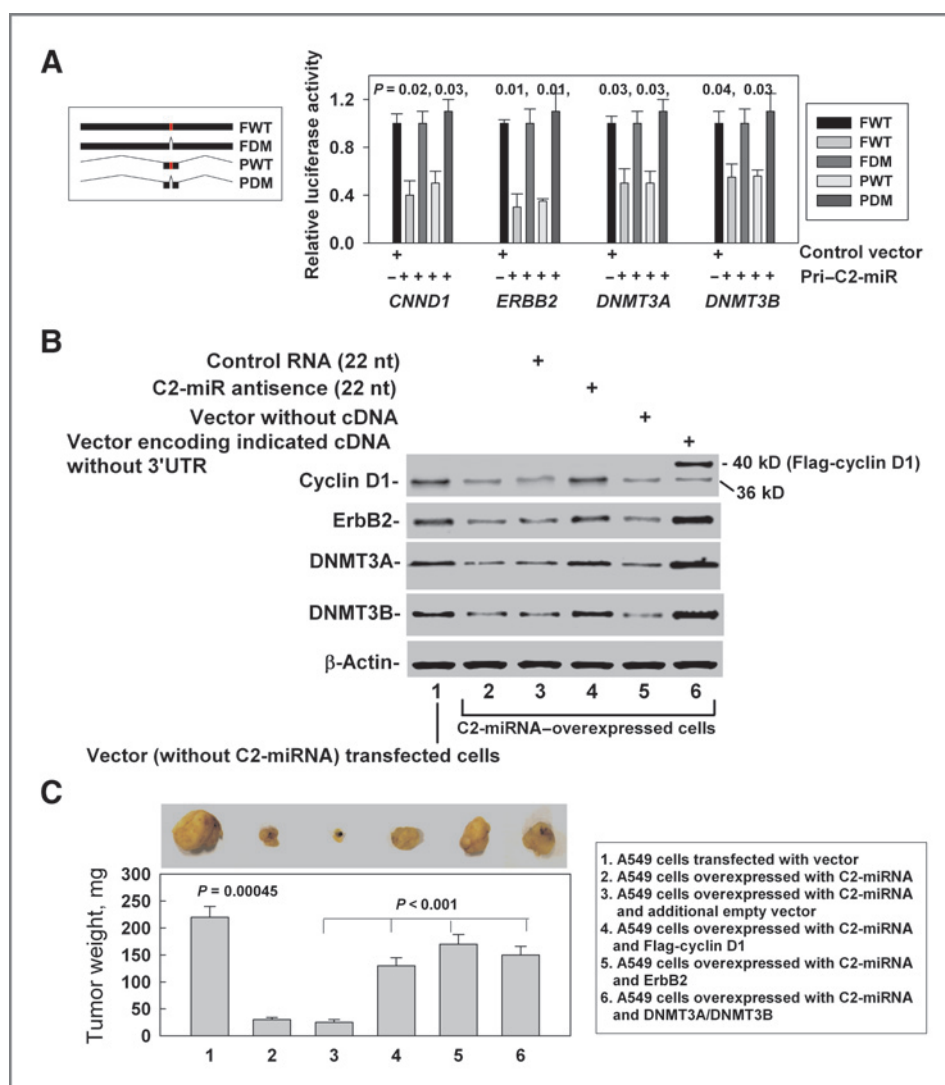


**Figure 5.** C2-miRNA inhibits human tumor cell growth through targeting *CCND1*, *ERBB2*, *DNMT3A*, and *DNMT3B*. **A**, left, illustration of the 3'UTR reporters: FWT, full-length wild-type; FDM, full-length deletion (6–10 bp at the key binding site) mutant; PWT, partial wild-type (containing the key binding site); PDM, partial deletion (6–10 bp at the key binding site) mutant. Right, C2-miRNA specifically represses its targets in the luciferase assay in 293FT cells. Data, mean  $\pm$  SD from three independent experiments. **B**, the protein levels of cyclin D1, ErbB2, DNMT3A, and DNMT3B were measured from A549 cells transfected with an empty vector (lane 1), stably overexpressed with C2-miRNA (lane 2), the C2-miRNA-overexpressed cells treated with control RNA (lane 3) or with C2-miRNA inhibitor (lane 4), the C2-miRNA-overexpressed cells transfected with empty vector (lane 5) or with the vector encoding *CCND1*, *ERBB2*, *DNMT3A*, or *DNMT3B* without 3'UTR of the gene (lane 6). The cells overexpressed with vector encoding *FLAG-CCND1* (row 1, lane 6) were described in detail in Supplementary Fig. S5C. **C**, analysis of the tumor weight. The xenograft tumors derived from A549 cell lines (1, transfected with vector alone; 2, overexpressed with pri-C2-miRNA; 3, overexpressed with pri-C2-miRNA and an additional empty vector; 4, overexpressed with pri-C2-miRNA and Flag-cyclin D1; 5, overexpressed with pri-C2-miRNA and ErbB2; 6, overexpressed with pri-C2-miRNA and DNMT3A/DNMT3B). The tumors were weighed and the data represented as mean  $\pm$  SD from 5 tumors for each cell line.

$\geq 50\%$  sequence identity over the full length of the canonical hsa-miR-548 sequence (Supplementary Methods and Supplementary Fig. S6B). These results strongly support that although the expression levels of the miR-548 family members are much lower than the regular miRNAs in human cells, this miRNA family with its >1,000 members could have an important biologic effect on suppressing tumors through an accumulation of their members.

To find out whether other members of the miR-548 family could be similar to C2-miRNA to target the same oncogenes, we

examined the effects of 36 commercially (GeneCopoeia) available plasmids encoding GFP and 36 individual members of the miR-548 family on the ErbB2 levels in 293FT cells after the cells were transfected with the plasmid. The results showed that among the 36 member (of the miR-548 family) upregulated cells, 19 of them showed lower ErbB2 expression than GFP vector alone-transfected cells (Supplementary Fig. S6C), supporting the conservative target of the miR-548 family. On the basis of these results, we further examined the effects of the 19 members of the miR-548 family on the levels of cyclin D1,

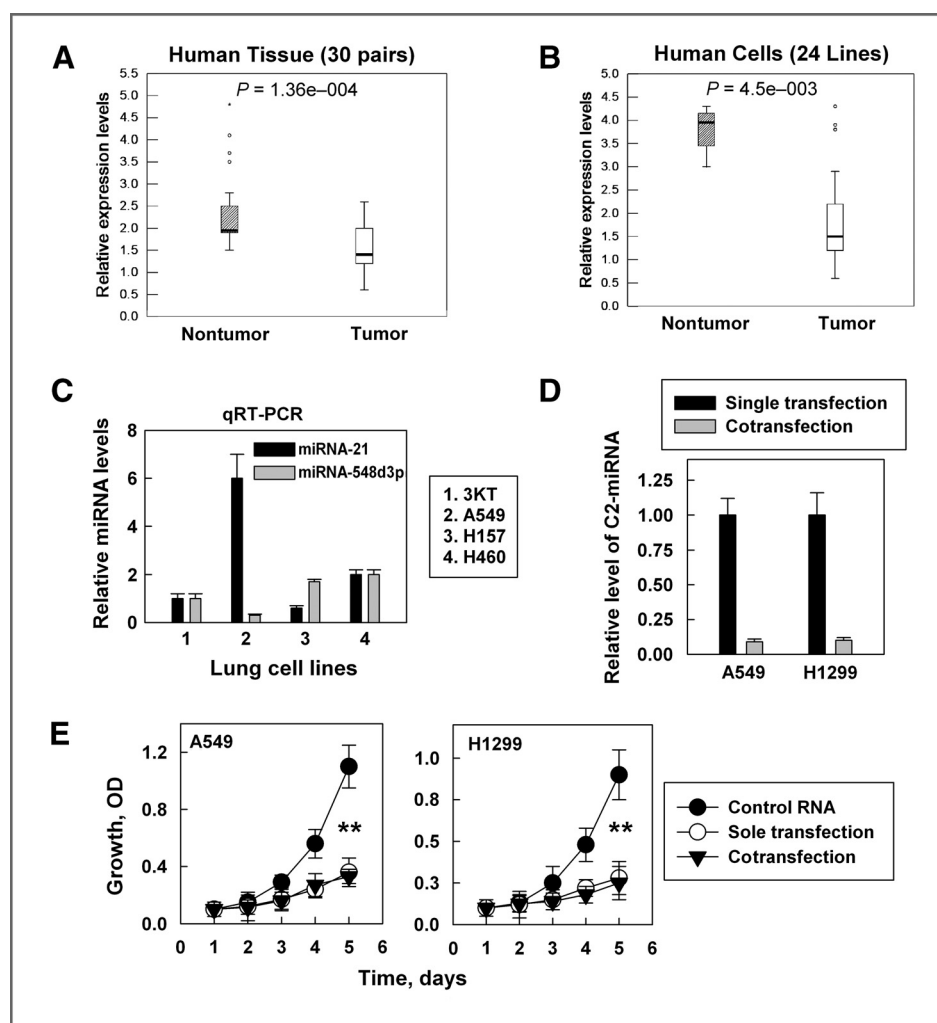


**Figure 6.** The important accumulative effects of the miR-548 family on inhibiting human tumor cell growth. A, the relative levels of the sum of 19 members of the miR-548 family (representing 29 mature miR-548 members) in 30 pairs of human lung cancer tissue and their adjacent nontumor tissue were measured by using NanoString technology (Supplementary Fig. S6A). B, the relative levels of the sum of the miR-548 family members in 24 human cell lines (5 normal and 19 tumor cell lines) were measured using NanoString technology (Supplementary Fig. S6A). C, the relative expression levels of miR-21 and miR-548d-3p (ratio of other cell lines to 3KT) were measured by qRT-PCR with the proper primers (purchased from ABI Inc.). D, the levels of C2-miRNA in A549 cells that were transiently transfected with the control RNA (30 nmol/L), the C2-miRNA mimic alone (30 nmol/L), or a mimic mixture of 10 miRNAs, including C2-miRNA and other 9 members of miR-548 family (miR-548a, miR-548d, miR-548e, miR-548f, miR-548i, miR-548h, miR-548o, miR-548s, and miR-548t), respectively (3 nmol/L for each one and total 30 nmol/L), were measured by qRT-PCR. The control RNA and all the mimics of the miR-548 family members (including C2-miRNA) were purchased from ABI Inc. Data, mean  $\pm$  SD from three independent experiments with triple samples for each experiment. E, cell viability of these cells as described in D was measured. The experiments were similar as described in Fig. 4A–C. Data, mean  $\pm$  SD from three independent experiments; \*\*,  $P < 0.01$ .

ErbB2, and DNMT3B after transfecting them into A549 cells. The results showed that the lower expressions of ErbB2, cyclin D1, and DNMT3B were observed in most samples after the cells were transfected with the miR-548 members (Supplementary Fig. S6D). These results demonstrate that different members of the miR-548 family could target the same oncogenes, suggesting an accumulative effect of the miR-548 family on inhibiting human tumor development.

To verify the hypothesis, we compared the growth change in A549 or H1299 human tumor cell lines that were solely transfected with C2-miRNA alone or cotransfected with the 10 miRNAs (the C2-miRNA amount in the cotransfection

mixture was 1/10 of the amount in the sole transfection). The results showed that although the C2-miRNA level in the cells cotransfected with the 10 miRNA mixture was only 1/10 of that in the cells solely transfected with C2-miRNA (Fig. 6D), the inhibitory effects of C2-miRNA on tumor cell growth were comparable between the cells solely transfected with C2-miRNA or cotransfected with the 10 miRNA mixture (Fig. 6E). These results strongly support that C2-miRNA could play an accumulative role with other members of the miR-548 family in inhibiting tumor cell growth, suggesting the importance of the miR-548 family in suppressing tumor development.

## Discussion

*FHIT* is located at *FRA3B* (1) that is a common fragile site. Fragile sites have been associated with genome instability in cancer cells, such as deletion, chromatin translocation, and the activation of the DNA damage response to stalled replication. Deletions of *FHIT*, including deletions of hundreds of kilobase, or copy-number alterations, within the gene are frequently found in *FRA3B/FHIT* in solid tumors; therefore, as an *FHIT* intron miRNA, the C2-miRNA expression level might be affected by a deletion in the related genomic region. The same expression trend of *Fhit* and C2-miRNA in the tumor samples from our data strongly supports such statement. Previously, many important genes related to the fragile site have been identified. Now, the importance of miRNA in the fragile sites has been realized (17, 44). Identifying a new member of the miR-548 family in the *FHIT* intron, as described in this study, adds importance to *FHIT* as an important tumor suppressor at the fragile site.

Our results suggest that the relatively low levels of mature miR-548 members are not due to the transcription regulation but are related to the inefficient RNase processes. The inefficient RNase process might be related to the 3' or 5' repeated "A" or "U" in the sequence of the miR-548 family members. However, the mechanism involved in whether the process from pri-miRNA to pre-miRNA or the process from pre-miRNA to mature miRNA needs the future experiments to elucidate. Hsa-miR-548 is a multicopy family of human miRNA genes. The expression levels of the mature miR-548 members are relatively low when compared with most other miRNAs in the human genome, for example, the CT value for miR-21 is approximately 26, for miR-34 is approximately 32, and for C2-miRNA is approximately 35 in 293FT cells measured by a RT-PCR approach. However, the miR-548 family members working on their targets are efficient as shown in this study, approximately 20-folds of relative level of exogenous upregulated C2-miRNA in HeLa cells (Fig. 1E) efficiently inhibited the tumor cell growth (Fig. 4C and E). In fact, close to 8,000 *Made1* are derived sequences in the human genome, and there are >1,000 sequences with >50% sequence identities over the full length of the canonical miR-548 sequence. Thus, it is reasonable that the aggregate expression of multiple family members may exert

substantial regulatory effects on host gene targets. The results in Fig. 6A and B indicate that similar to C2-miRNA, the known miR-548 family members in lung tumors also expressed lower than in their adjacent nontumor tissues. The reason why the sum of other known members of the miR-548 family was lower in lung tumors than in their adjacent nontumor tissues remains unclear; however, the fact that many miR-548 family members locate in fragile sites might partially explain the low expression of the miR-548 family. It is worthy in the future to explore the nature of lower expression of the miR-548 family in tumor than in normal tissue. Taken together, it is expected that the miR-548 family could be either used as a useful parameter to evaluate the progress of human tumors or developed into new therapeutic reagents for cancer treatment.

## Disclosure of Potential Conflicts of Interest

No potential conflicts of interest were disclosed.

## Authors' Contributions

**Conception and design:** B. Hu, P. Zhao, W.J. Curran, Y. Wang  
**Development of methodology:** B. Hu, X. Ying, J. Wang, I.K. Jordan, P. Zhao, W.L. Ng, Y. Wang  
**Acquisition of data (provided animals, acquired and managed patients, provided facilities, etc.):** B. Hu, J. Wang, J. Piriyaopongsa, I.K. Jordan, J. Sheng, F. Yu, P. Zhao, Y. Li, H. Wang, C. Wang, W. Li, Y. Wang  
**Analysis and interpretation of data (e.g., statistical analysis, biostatistics, computational analysis):** X. Ying, J. Wang, J. Piriyaopongsa, I.K. Jordan, P. Zhao, S. Hu, Y. Wang  
**Writing, review, and/or revision of the manuscript:** X. Ying, P. Zhao, W.J. Curran, Y. Wang  
**Administrative, technical, or material support (i.e., reporting or organizing data, constructing databases):** J. Piriyaopongsa, P. Zhao, X. Wang  
**Study supervision:** B. Hu, W.J. Curran, Y. Wang

## Acknowledgments

The authors thank Drs. Joan Allalunis-Turner, Yinglin Lu, and Shi-Yong Sun for providing cell lines; members of the Wang laboratory for helpful discussion; and Doreen Theune for editing the article.

## Grant Support

This work was supported by Emory start-up funds and the National Natural Sciences Foundation of China (31070760, 30770651, and 30670616).

The costs of publication of this article were defrayed in part by the payment of page charges. This article must therefore be hereby marked *advertisement* in accordance with 18 U.S.C. Section 1734 solely to indicate this fact.

Received November 18, 2013; revised January 23, 2014; accepted February 6, 2014; published OnlineFirst February 20, 2014.

## References

- Ohta M, Inoue H, Cotticelli MG, Kastury K, Baffa R, Palazzo J, et al. The *FHIT* gene, spanning the chromosome 3p14.2 fragile site and renal carcinoma-associated t(3;8) breakpoint, is abnormal in digestive tract cancer. *Cell* 1996;84:587-97.
- Sozzi G, Torioli S, Tagliabue E, Sard L, Pezzella F, Patorino U, et al. Absence of *Fhit* protein in primary lung tumors and cell lines with *FHIT* gene abnormalities. *Cancer Res* 1997;57:5207-12.
- Burke L, Khan MA, Freedman AN, Gemma A, Rusin M, Guinee DG, et al. Allelic deletion analysis of the *FHIT* gene predicts poor survival in non-small cell lung cancer. *Cancer Res* 1998;58:2533-6.
- Sozzi G, Patorino U, Moiraghi L, Tagliabue E, Pezzella F, Ghirelli C, et al. Loss of *FHIT* function in lung cancer and preinvasive bronchial lesions. *Cancer Res* 1998;58:5032-7.
- Krivak TC, McBroom JW, Seidman J, Venzon D, Crothers B, MacKoul PJ, et al. Abnormal Fragile Histidine Triad (*FHIT*) expression in advanced cervical carcinoma. *Cancer Res* 2001;61:4382-5.
- Takizawa S, Nakagawa S, Nakagawa K, Yasugi T, Fujii T, Kugu K, et al. Abnormal *Fhit* expression is an independent poor prognostic factor for cervical cancer. *Br J Cancer* 2003;88:1213-6.
- Zhao P, Liu W, Lu Y-L. Clinicopathological significance of *FHIT* protein expression in gastric adenocarcinoma patients. *World J Gastroenterol* 2005;11:5735-8.
- Fong LYY, Fidanza V, Zanesi N, Lock LF, Siracusa LD, Mancini R, et al. Muir-Torre-like syndrome in *Fhit*-deficient mice. *Proc Natl Acad Sci U S A* 2000;97:4742-7.

9. Pekarsky Y, Garrison PN, Palamarchuk A, Zaneni N, Aqeilan RI, Huebner K, et al. Fhit is a physiological target of the protein kinase Src. *Proc Natl Acad Sci U S A* 2004;101:3775–9.
10. Ishii H, Mimori K, Inoue H, Inageta T, Ishikawa K, Semba S, et al. Fhit modulates the DNA damage checkpoint response. *Cancer Res* 2006;66:11287–92.
11. Trapasso F, Pichiorri F, Gaspari M, Palumbo T, Aqeilan RI, Gaudio E, et al. Fhit interaction with ferredoxin reductase triggers generation of reactive oxygen species and apoptosis of cancer cells. *J Biol Chem* 2008;283:13736–44.
12. Saldivar JC, Shibata H, Huebner K. Pathology and biology associated with the fragile FHIT gene and gene product. *J Cell Biochem* 2010;109:858–65.
13. Siprashvili Z, Sozzi G, Barnes LD, McCue P, Robinson AK, Eryomin V, et al. Replacement of Fhit in cancer cells suppresses tumorigenicity. *Proc Natl Acad Sci U S A* 1997;94:13771–6.
14. Mao L. Tumor suppressor genes: does FHIT fit? *J Natl Cancer Inst* 1998;90:412–4.
15. Otterson GA, Chen W-d, Niklinska W, Kaye FJ, Xiao G-H, Jin F, et al. Protein expression and functional analysis of the FHIT gene in human tumor cells. *J Natl Cancer Inst* 1998;90:426–32.
16. Ji L, Fang B, Yen N, Fong K, Minna JD, Roth JA. Induction of apoptosis and inhibition of tumorigenicity and tumor growth by adenovirus vector-mediated fragile histidine triad (FHIT) gene overexpression. *Cancer Res* 1999;59:3333–9.
17. Calin G, Sevignani C, Dumitru C, Hyslop T, Noch E, Yendamuri S, et al. Human microRNA genes are frequently located at fragile sites and genomic regions involved in cancers. *Proc Natl Acad Sci U S A* 2004;101:2999–3004.
18. Piriyaopongsa J, Jordan IK. A family of human microRNA genes from miniature inverted-repeat transposable elements. *PLoS ONE* 2007;2:e203.
19. Yuan Z, Sun X, Liu H, Xie J. MicroRNA genes derived from repetitive elements and expanded by segmental duplication events in mammalian genomes. *PLoS ONE* 2011;6:e17666.
20. Rhead B, Karolchik D, Kuhn RM, Hinrichs AS, Zweig AS, Fujita PA, et al. The UCSC Genome Browser database: update 2010. *Nucleic Acids Res* 2010;38:D613–9.
21. Griffiths-Jones S, Grocock RJ, van Dongen S, Bateman A, Enright AJ. miRBase: microRNA sequences, targets and gene nomenclature. *Nucleic Acids Res* 2006;34:D140–4.
22. Hofacker I, Fontana W, Stadler P, Bonhoeffer L, Tacker M, Schuster P. Fast folding and comparison of RNA secondary structures. *Monatshfte Für Chemie* 1994;125:167–88.
23. Griffiths-Jones S. miRBase: microRNA sequences and annotation. *Curr Protoc Bioinformatics* 2010;29:12.9.1–12.9.10.
24. Mituyama T, Yamada K, Hattori E, Okida H, Ono Y, Terai G, et al. The Functional RNA Database 3.0: databases to support mining and annotation of functional RNAs. *Nucleic Acids Res* 2009;37:D89–92.
25. He M, Stoevesandt O, Palmer EA, Khan F, Ericsson O, Taussig MJ. Printing protein arrays from DNA arrays. *Nat Methods* 2008;5:175–7.
26. Yan D, Ng W, Zhang X, Wang P, Zhang Z, Mo Y, et al. Targeting DNA-PK and ATM with miR-101 sensitizes tumors to radiation. *PLoS ONE* 2010;5:e11397.
27. Zhu Y, Yu X, Fu H, Wang H, Wang P, Zheng X, et al. MicroRNA-21 involves radiation-promoted liver carcinogenesis. *Int J Clin Exp Med* 2010;3:211–22.
28. Ramirez RD, Sheridan S, Girard L, Sato M, Kim Y, Pollack J, et al. Immortalization of human bronchial epithelial cells in the absence of viral oncoproteins. *Cancer Res* 2004;64:9027–34.
29. Allalunis-Turner MJ, Barron GM, Day RS, Dobler KD, Mirzayans R. Isolation of two cell lines from a human malignant glioma specimen differing in sensitivity to radiation and chemotherapeutic drugs. *Radiat Res* 1993;134:349–54.
30. Kim KB, Lotan R, Yue P, Sporn MB, Suh N, Gribble GW, et al. Identification of a novel synthetic triterpenoid, methyl-2-cyano-3,12-dioxooleana-1,9-dien-28-oate, that potently induces caspase-mediated apoptosis in human lung cancer cells. *Mol Cancer Ther* 2002;1:177–84.
31. Lu L, Hu B, Yu F, Wang Y. Low dose radiation-induced adaptive response preventing HPRT mutation is Fhit independent. *Int J Radiat Biol* 2009;85:532–7.
32. Fu HJ, Zhu J, Yang M, Zhang ZY, Tie Y, Jiang H, et al. A novel method to monitor the expression of microRNAs. *Mol Biotechnol* 2006;32:197–204.
33. Christman JK. 5-Azacytidine and 5-aza-2'-deoxycytidine as inhibitors of DNA methylation: mechanistic studies and their implications for cancer therapy. *Oncogene* 2002;21:5483–95.
34. Zöchbauer-Müller S, Fong KM, Maitra A, Lam S, Geradts J, Ashfaq R, et al. 5' CpG island methylation of the FHIT gene is correlated with loss of gene expression in lung and breast cancer. *Cancer Res* 2001;61:3581–5.
35. Forbes SA, Bindal N, Bamford S, Cole C, Kok CY, Beare D, et al. COSMIC: mining complete cancer genomes in the catalogue of somatic mutations in Cancer. *Nucleic Acids Res* 2011;39:D945–50.
36. Zhao P, Lu Y, Zhong M, Liu L, Li B. Inverse correlation of aberrant expression of fragile histidine triad (FHIT) protein with cyclin D1 protein and prognosis in Chinese patients with cholangiocarcinoma. *Acta Oncol* 2008;47:1557–63.
37. Chen H, Sun Jg, Cao X-w, Ma X-g, Xu J-p, Luo F-k, et al. Preliminary validation of ERBB2 expression regulated by miR-548d-3p and miR-559. *Biochem Biophys Res Comm* 2009;385:596–600.
38. Yu Z, Wang C, Wang M, Li Z, Casimiro MC, Liu M, et al. A cyclin D1/microRNA 17/20 regulatory feedback loop in control of breast cancer cell proliferation. *J Cell Biol* 2008;182:509–17.
39. Chen J, Feilolter HE, Pare GC, Zhang X, Pemberton JG, Garady C, et al. MicroRNA-193b represses cell proliferation and regulates cyclin D1 in melanoma. *Am J Pathol* 2010;176:2520–9.
40. Sassen S, Miska EA, Caldas C. MicroRNA: implications for cancer. *Virchows Arch* 2008;452:1–10.
41. Fabbri M, Garzon R, Cimmino A, Liu Z, Zaneni N, Callegari E, et al. MicroRNA-29 family reverts aberrant methylation in lung cancer by targeting DNA methyltransferases 3A and 3B. *Proc Natl Acad Sci U S A* 2007;104:15805–10.
42. Wu S, Huang S, Ding J, Zhao Y, Liang L, Liu T, et al. Multiple microRNAs modulate p21Cip1/Waf1 expression by directly targeting its 3' untranslated region. *Oncogene* 2010;29:2302–8.
43. Geiss GK, Bumgarner RE, Birditt B, Dahl T, Dowidar N, Dunaway DL, et al. Direct multiplexed measurement of gene expression with color-coded probe pairs. *Nat Biotechnol* 2008;26:317–25.
44. Croce CM. miRNAs in the spotlight: understanding cancer gene dependency. *Nat Med* 2011;17:935–6.
45. Zhang X, Ng W-L, Wang P, Tian L, Werner E, Wang H, et al. MicroRNA-21 modulates the levels of reactive oxygen species by targeting SOD3 and TNF $\alpha$ . *Cancer Res* 2012;72:4707–13.